

# Quantifying Coherence-to-Entanglement Conversion Efficiency under Noisy Operations

Asad Ali<sup>1,\*</sup>, H. Kuniyil<sup>1</sup>, M.I Hussain<sup>1</sup>, M.T Rahim<sup>1</sup>, Abdallah Slaoui<sup>2,3</sup> and Saif Al-Kuwari<sup>1,†</sup>

<sup>1</sup>*Qatar Center for Quantum Computing, College of Science and Engineering, Hamad Bin Khalifa University, Doha, Qatar*

<sup>2</sup>*LPHE-Modelling and Simulation, Faculty of Sciences,  
Muhammad V University in Rabat, Rabat, Morocco*

<sup>3</sup>*Centre of Physics and Mathematics, CPM, Faculty of Sciences,  
Muhammad V University in Rabat, Rabat, Morocco*

(Dated: June 16, 2026)

We investigate the noise-limited conversion of local quantum coherence into bipartite entanglement in a minimal two-qubit protocol comprising a coherent single-qubit input, an incoherent ancilla, an ideal CNOT operation, and subsequent environmental noise. Employing the  $l_1$ -norm of coherence and the entanglement negativity as resource quantifiers, we establish an exact closed-form correspondence between local single-qubit input coherence and the two-qubit entanglement generated in the noiseless limit, showing that the output negativity is precisely one half of the initial  $l_1$ -coherence. We then derive analytic expressions for the surviving entanglement and the associated coherence-to-entanglement conversion efficiency under two representative noise mechanisms: independent phase damping and global two-qubit depolarizing noise. The two channels exhibit qualitatively distinct degradation behavior. Phase damping induces a universal multiplicative suppression of the generated entanglement, yielding a coherence-independent conversion efficiency and no finite-noise entanglement sudden death. In contrast, global depolarization introduces an isotropic mixing contribution that shifts the partial-transpose spectrum, producing coherence-dependent degradation and a finite sudden-death threshold. We show that maximally coherent inputs not only maximize the entanglement generated by the CNOT protocol but also optimize its robustness against depolarizing noise. Direct density-matrix simulations validate the analytic results to numerical precision. These findings provide a compact analytic benchmark for assessing how different noise mechanisms constrain coherence-to-entanglement conversion in elementary quantum-information protocols and near-term quantum devices.

## I. INTRODUCTION

Quantum coherence and entanglement are two fundamental resources in quantum information science. Coherence quantifies the ability of a quantum system to exist in superposition with respect to a fixed reference basis, whereas entanglement describes nonclassical correlations shared between distinct subsystems. Both resources play a central role in quantum computation, communication, metrology, thermodynamics, and quantum technologies [1–10]. The resource theory of quantum coherence, formalized by Baumgratz, Cramer, and Plenio [3], introduced coherence monotones such as the  $l_1$ -norm of coherence and the relative entropy of coherence. Subsequent developments clarified the operational role of coherence and its connections with other forms of nonclassicality, particularly entanglement [4, 11].

A key result in this direction is that local coherence can be converted into bipartite entanglement by coupling the coherent system to an initially incoherent ancilla through an incoherent operation [3, 11]. A minimal example of such a conversion is provided by the controlled-NOT (CNOT) gate. If qubit  $A$  is prepared in the coherent state  $|\psi_A\rangle = \cos\theta|0\rangle + e^{i\phi}\sin\theta|1\rangle$  and qubit  $B$  is initial-

ized in the incoherent state  $|0\rangle$ , then a CNOT gate with  $A$  as the control and  $B$  as the target produces

$$|\Psi\rangle_{AB} = \cos\theta|00\rangle + e^{i\phi}\sin\theta|11\rangle.$$

Thus, the local coherence initially stored in a single qubit is converted into nonlocal quantum correlations between two qubits. For  $\theta = \pi/4$ , the output is maximally entangled, while for  $\theta = 0$  or  $\theta = \pi/2$ , the input is incoherent in the computational basis and no entanglement is generated. This makes the CNOT protocol one of the simplest analytically tractable settings for studying coherence-to-entanglement conversion.

However, in realistic quantum devices, entanglement generation is inevitably affected by environmental noise and operational imperfections. Dephasing, depolarization, relaxation, imperfect control, and other noise processes can degrade the quantum resources produced by a circuit [12, 13]. The degradation of entanglement under noise is a well-established topic, including the phenomenon of entanglement sudden death, in which an initially entangled state becomes separable at a finite noise strength or finite time [14]. The negativity, introduced by Vidal and Werner and further discussed in later reviews [15, 16], provides a convenient entanglement monotone based on the spectrum of the partially transposed density matrix. For two-qubit systems, it is especially useful because positivity of the partial transpose is both necessary and sufficient for separability.

\* asal68826@hbku.edu.qa

† smalkuwari@hbku.edu.qa

Although coherence-to-entanglement conversion and entanglement degradation under noise have both been widely studied, it is useful to have compact closed-form benchmarks that directly connect the coherence of the input state with the entanglement that survives after a noisy conversion process. Such benchmarks are valuable because they isolate the role of specific noise mechanisms and provide simple reference formulas against which more complex protocols, noise models, or device-level simulations can be compared. In particular, the elementary CNOT protocol allows the conversion process to be quantified directly in terms of the input  $l_1$ -norm coherence and the output negativity, while retaining a density-matrix structure simple enough to permit exact analytic treatment.

In this work, we analyze noise-limited coherence-to-entanglement conversion in this minimal two-qubit setting. We consider a coherent single-qubit input, an ancillary qubit initialized in  $|0\rangle$ , an ideal CNOT gate, and a noise channel applied to the resulting two-qubit state. Two canonical one-parameter noise models are studied. The first is independent phase damping on both qubits, which suppresses off-diagonal density-matrix elements while preserving populations. The second is the global two-qubit depolarizing channel, which mixes the state isotropically with the maximally mixed state. These channels represent physically distinct degradation mechanisms: phase damping removes phase coherence without population mixing, whereas global depolarization introduces isotropic mixing over the full two-qubit Hilbert space.

Using the restricted  $X$ -state structure generated by the CNOT protocol, we compute the partial transpose explicitly and derive closed-form expressions for the output negativity under both noise models. In the ideal case, the output negativity is half of the input  $l_1$ -norm coherence. Under independent phase damping, the generated entanglement decays multiplicatively, leading to a conversion efficiency that is independent of the initial coherence angle. By contrast, under global two-qubit depolarizing noise, the isotropic identity contribution shifts the partial-transpose spectrum and produces a finite entanglement sudden-death threshold. The resulting analysis provides a simple closed-form comparison between dephasing-induced coherence suppression and depolarization-induced separability in a CNOT-based coherence-to-entanglement conversion protocol.

The remainder of the paper is organized as follows. Section II introduces the input state, the  $l_1$ -norm coherence, and the negativity as the entanglement measure. Section III analyzes the ideal CNOT conversion and derives the coherence-entanglement proportionality. Section IV defines the independent phase-damping and global depolarizing channels used in the analysis. Section V develops the partial-transpose calculation for the relevant  $X$ -state structure. Sections VI and VII derive the exact negativities under phase damping and global depolarizing noise, respectively. Section VIII analyzes

the depolarizing entanglement sudden-death threshold, while Section IX discusses coherence-to-entanglement conversion efficiency. Numerical validation is presented in Section XI, followed by discussion and conclusions in Sections XII and XIII, respectively.

## II. THEORETICAL FRAMEWORK

### A. System and Initial State

We consider a two-qubit system composed of qubits  $A$  and  $B$ , with Hilbert spaces  $\mathcal{H}_A \cong \mathbb{C}^2$  and  $\mathcal{H}_B \cong \mathbb{C}^2$ . The joint Hilbert space is  $\mathcal{H}_{AB} = \mathcal{H}_A \otimes \mathcal{H}_B \cong \mathbb{C}^4$ . Throughout the paper, we use the computational basis  $\{|00\rangle, |01\rangle, |10\rangle, |11\rangle\}$ .

Qubit  $A$  is initialized in the pure coherent state

$$|\psi_A\rangle = \cos\theta |0\rangle + e^{i\phi} \sin\theta |1\rangle, \quad \theta \in \left[0, \frac{\pi}{2}\right], \quad \phi \in [0, 2\pi), \quad (1)$$

with density operator  $\rho_A = |\psi_A\rangle\langle\psi_A|$ . The parameter  $\theta$  controls the population imbalance, while  $\phi$  is the relative phase. Qubit  $B$  is initialized in the incoherent reference state

$$\rho_B = |0\rangle\langle 0| = \begin{pmatrix} 1 & 0 \\ 0 & 0 \end{pmatrix}. \quad (2)$$

The initial two-qubit state is therefore the product state

$$\rho_0 = \rho_A \otimes \rho_B = |\psi_A\rangle\langle\psi_A| \otimes |0\rangle\langle 0|. \quad (3)$$

At this stage, the state contains local coherence in qubit  $A$  but no entanglement between  $A$  and  $B$ .

### B. Quantum Coherence Measure

We quantify the coherence of qubit  $A$  using the  $l_1$ -norm of coherence, defined with respect to the computational basis as [3]

$$C_{l_1}(\rho_A) = \sum_{i \neq j} |\rho_{ij}|. \quad (4)$$

For the pure state in Eq. (1), the only off-diagonal elements of  $\rho_A$  are  $\rho_{01} = e^{-i\phi} \cos\theta \sin\theta$  and  $\rho_{10} = e^{i\phi} \cos\theta \sin\theta$ . Hence,

$$C_{l_1}(|\psi_A\rangle) = 2|\cos\theta \sin\theta| = \sin(2\theta), \quad (5)$$

where the final equality follows from  $\theta \in [0, \pi/2]$ . The coherence is maximal at  $\theta = \pi/4$ , where  $C_{l_1} = 1$ , and vanishes at  $\theta = 0$  and  $\theta = \pi/2$ , where the input state is a computational basis state.

### C. Entanglement Measure

We quantify bipartite entanglement using the negativity [15, 16]. For a two-qubit density operator  $\rho_{AB}$ , the negativity is defined as

$$\mathcal{N}(\rho_{AB}) = \frac{\|\rho_{AB}^{T_B}\|_1 - 1}{2}, \quad (6)$$

where  $\rho_{AB}^{T_B}$  denotes the partial transpose with respect to subsystem  $B$ , and  $\|\cdot\|_1$  is the trace norm. In the computational basis, the partial transpose is defined by

$$\langle i, j | \rho_{AB}^{T_B} | k, l \rangle = \langle i, l | \rho_{AB} | k, j \rangle, \quad (7)$$

with  $i, j, k, l \in \{0, 1\}$ . Equivalently, if  $\{\lambda_i\}$  are the eigenvalues of  $\rho_{AB}^{T_B}$ , then

$$\mathcal{N}(\rho_{AB}) = \sum_{\lambda_i < 0} |\lambda_i|. \quad (8)$$

For two-qubit systems, positivity of the partial transpose is necessary and sufficient for separability. Therefore,  $\mathcal{N}(\rho_{AB}) > 0$  is equivalent to entanglement in the present setting.

## III. IDEAL CONVERSION PROTOCOL

### A. CNOT Gate Action

We first analyze the noiseless coherence-to-entanglement conversion induced by the CNOT gate. The control qubit is  $A$ , and the target qubit is  $B$ . The action of the CNOT gate on the computational basis is

$$U_{\text{CNOT}} |a, b\rangle = |a, a \oplus b\rangle, \quad (9)$$

where  $a, b \in \{0, 1\}$  and  $\oplus$  denotes addition modulo two. In the ordered basis  $\{|00\rangle, |01\rangle, |10\rangle, |11\rangle\}$ , the matrix representation is

$$U_{\text{CNOT}} = \begin{pmatrix} 1 & 0 & 0 & 0 \\ 0 & 1 & 0 & 0 \\ 0 & 0 & 0 & 1 \\ 0 & 0 & 1 & 0 \end{pmatrix}. \quad (10)$$

Applying this unitary to the initial product state  $|\psi_A\rangle \otimes |0\rangle$  gives

$$\begin{aligned} |\Psi\rangle &= U_{\text{CNOT}} (\cos\theta |0\rangle + e^{i\phi} \sin\theta |1\rangle) \otimes |0\rangle \\ &= \cos\theta |00\rangle + e^{i\phi} \sin\theta |11\rangle. \end{aligned} \quad (11)$$

Thus, the initial local coherence of qubit  $A$  is converted into nonlocal coherence between  $|00\rangle$  and  $|11\rangle$ . For  $\theta \in (0, \pi/2)$ , the output state has Schmidt rank two and is entangled.

The corresponding density operator is

$$\rho = |\Psi\rangle\langle\Psi| = \begin{pmatrix} a & 0 & 0 & c \\ 0 & 0 & 0 & 0 \\ 0 & 0 & 0 & 0 \\ c^* & 0 & 0 & b \end{pmatrix}, \quad (12)$$

where

$$a = \cos^2\theta, \quad b = \sin^2\theta, \quad c = e^{-i\phi} \cos\theta \sin\theta = \frac{1}{2} e^{-i\phi} \sin(2\theta). \quad (13)$$

The state has a restricted  $X$ -state structure: only the diagonal populations  $\rho_{11}$ ,  $\rho_{44}$  and the anti-diagonal coherence  $\rho_{14}$ ,  $\rho_{41}$  are nonzero. This simple structure is the key reason why the negativity can be obtained in closed form.

### B. Ideal Negativity and Coherence-Entanglement Relation

To compute the ideal output entanglement, we take the partial transpose with respect to subsystem  $B$ . Using Eq. (7), the partial transpose of  $\rho$  is

$$\rho^{T_B} = \begin{pmatrix} a & 0 & 0 & 0 \\ 0 & 0 & c & 0 \\ 0 & c^* & 0 & 0 \\ 0 & 0 & 0 & b \end{pmatrix}. \quad (14)$$

This matrix consists of two one-dimensional blocks with eigenvalues  $a$  and  $b$ , and one  $2 \times 2$  block,

$$\begin{pmatrix} 0 & c \\ c^* & 0 \end{pmatrix}, \quad (15)$$

whose eigenvalues are  $\pm|c|$ . Hence, the full spectrum of  $\rho^{T_B}$  is

$$\lambda_1 = a = \cos^2\theta, \quad \lambda_2 = b = \sin^2\theta, \quad \lambda_{\pm} = \pm|c| = \pm\frac{1}{2} \sin(2\theta). \quad (16)$$

the only negative eigenvalue is  $\lambda_- = -\frac{1}{2} \sin(2\theta)$ . Therefore, the ideal negativity is

$$\mathcal{N}_0(\theta) = \frac{1}{2} \sin(2\theta). \quad (17)$$

Comparing this expression with the input coherence  $C_{l_1}(|\psi_A\rangle) = \sin(2\theta)$ , obtained in Eq. (5), gives the following relation.

**Proposition 1.** *For the CNOT conversion protocol with input state  $|\psi_A\rangle = \cos\theta |0\rangle + e^{i\phi} \sin\theta |1\rangle$ , the noiseless output negativity is one half of the input  $l_1$ -norm coherence:*

$$\boxed{\mathcal{N}_0(\theta) = \frac{1}{2} C_{l_1}(|\psi_A\rangle)}. \quad (18)$$

*Proof.* The result follows directly from  $C_{l_1}(|\psi_A\rangle) = \sin(2\theta)$  and  $\mathcal{N}_0(\theta) = \frac{1}{2} \sin(2\theta)$ .  $\square$

This relation provides the noiseless reference point for the noisy protocols considered below. The numerical factor  $1/2$  is specific to using negativity as the entanglement measure. In particular, the maximum value  $\mathcal{N}_0 = 1/2$  is reached at  $\theta = \pi/4$ , where the input is maximally coherent and the CNOT output is the Bell state  $(|00\rangle + e^{i\phi}|11\rangle)/\sqrt{2}$ . At  $\theta = 0$  or  $\theta = \pi/2$ , the input is incoherent in the computational basis and the output remains separable.

#### IV. NOISE CHANNELS

After the CNOT operation, the two-qubit state is subjected to environmental noise, modeled by a completely positive trace-preserving (CPTP) map  $\mathcal{E}$ . We consider two standard one-parameter noise models: independent phase damping on both qubits and global two-qubit depolarizing noise. These channels capture two qualitatively different degradation mechanisms. Phase damping suppresses off-diagonal coherences while preserving populations, whereas global depolarizing noise mixes the state isotropically with the maximally mixed state.

##### A. Phase-Damping Channel

The single-qubit phase-damping channel is defined by the Kraus operators

$$K_0 = \begin{pmatrix} 1 & 0 \\ 0 & \sqrt{1-p} \end{pmatrix}, \quad K_1 = \begin{pmatrix} 0 & 0 \\ 0 & \sqrt{p} \end{pmatrix}, \quad (19)$$

where  $p \in [0, 1]$  is the dephasing strength. These operators satisfy  $\sum_k K_k^\dagger K_k = \mathbb{I}_2$ , so the map  $\mathcal{E}_{\text{phase}}(\rho) = \sum_k K_k \rho K_k^\dagger$  is CPTP. For a single-qubit density matrix, the channel acts as

$$\mathcal{E}_{\text{phase}} \left[ \begin{pmatrix} \rho_{00} & \rho_{01} \\ \rho_{10} & \rho_{11} \end{pmatrix} \right] = \begin{pmatrix} \rho_{00} & \sqrt{1-p} \rho_{01} \\ \sqrt{1-p} \rho_{10} & \rho_{11} \end{pmatrix}. \quad (20)$$

Thus, in this parametrization, single-qubit off-diagonal elements are suppressed by the factor  $\sqrt{1-p}$ , while populations are left unchanged. The limiting cases are  $p = 0$ , corresponding to the identity channel, and  $p = 1$ , corresponding to complete phase damping in the computational basis.

For the two-qubit system, we apply independent phase damping to qubits  $A$  and  $B$ . The two-qubit channel is therefore

$$\mathcal{E}_{\text{phase}}^{(2)} = \mathcal{E}_{\text{phase}} \otimes \mathcal{E}_{\text{phase}}, \quad (21)$$

with Kraus operators

$$K_{ij} = K_i \otimes K_j, \quad i, j \in \{0, 1\}. \quad (22)$$

Because the CNOT-generated entanglement is carried by the coherence between  $|00\rangle$  and  $|11\rangle$ , this two-qubit coherence is suppressed by a factor  $\sqrt{1-p} \times \sqrt{1-p} = 1-p$ . This convention for  $p$  will be used throughout the phase-damping analysis.

##### B. Global Depolarizing Channel

The second noise model is the global two-qubit depolarizing channel, defined by

$$\mathcal{E}_{\text{dep}}(\rho) = (1-p)\rho + \frac{p}{4}\mathbb{I}_4, \quad (23)$$

where  $p \in [0, 1]$ , and  $\mathbb{I}_4$  is the identity operator on the two-qubit Hilbert space. This channel interpolates between the identity map at  $p = 0$  and the completely mixed state  $\mathbb{I}_4/4$  at  $p = 1$ .

Unlike phase damping, the global depolarizing channel does not merely suppress coherences. Instead, it replaces the state with the maximally mixed state with probability  $p$ , thereby reducing all deviations from  $\mathbb{I}_4/4$ . In particular, off-diagonal elements are multiplied by  $(1-p)$ , while diagonal populations are shifted toward  $1/4$ . This isotropic mixing will be responsible for the finite entanglement sudden-death threshold derived below.

We emphasize that Eq. (23) describes a global two-qubit depolarizing channel. It is distinct from applying independent single-qubit depolarizing channels to qubits  $A$  and  $B$ , which would lead to a different density matrix and, in general, a different negativity expression.

#### V. RESTRICTED X-STATE STRUCTURE AND PARTIAL TRANSPOSE

The CNOT output in Eq. (12) has a restricted  $X$ -state structure, with nonzero elements only in the  $|00\rangle$  and  $|11\rangle$  subspace and in the coherence connecting these two basis states. This structure makes the partial-transpose spectrum especially simple. In this section, we first show how the restricted  $X$ -state form is preserved under the noise channels considered here, and then derive the corresponding partial-transpose eigenvalues used in the later calculations.

##### A. Preservation of the Restricted X-State Structure Under Noise

We begin with the noiseless CNOT output

$$\rho = \begin{pmatrix} a & 0 & 0 & c \\ 0 & 0 & 0 & 0 \\ 0 & 0 & 0 & 0 \\ c^* & 0 & 0 & b \end{pmatrix}, \quad (24)$$

where  $a = \cos^2 \theta$ ,  $b = \sin^2 \theta$ , and  $c = \frac{1}{2}e^{-i\phi} \sin(2\theta)$ .

For independent phase damping, diagonal elements are unchanged, while an off-diagonal element  $|x_{Ax_B}\rangle\langle y_{Ay_B}|$  is multiplied by one factor of  $\sqrt{1-p}$  for each qubit on which  $x$  and  $y$  differ. The only nonzero off-diagonal element of Eq. (24) is  $\rho_{14} = c$ , corresponding to  $|00\rangle\langle 11|$ . Since the two basis states differ in both qubits, this element transforms as

$$c \mapsto c_{\text{phase}} = (1-p)c, \quad (25)$$

while  $a$  and  $b$  are unchanged. Thus, the restricted  $X$ -state structure is preserved under independent phase damping.

For the global depolarizing channel,  $\mathcal{E}_{\text{dep}}(\rho) = (1-p)\rho + p\mathbb{I}_4/4$ . Since  $\mathbb{I}_4$  is diagonal in the computational basis, this channel also preserves the  $X$ -state form. However, unlike phase damping, it populates the  $|01\rangle$  and  $|10\rangle$  diagonal entries by adding  $p/4$  to each basis state. The resulting state is therefore still an  $X$ -state, but not of the restricted form in Eq. (24).

### B. Partial Transpose of the Restricted $X$ -State

Consider the restricted  $X$ -state

$$\rho_X = \begin{pmatrix} a' & 0 & 0 & c' \\ 0 & 0 & 0 & 0 \\ 0 & 0 & 0 & 0 \\ c'^* & 0 & 0 & b' \end{pmatrix}, \quad (26)$$

with  $a', b' \geq 0$ ,  $a' + b' = 1$ , and  $|c'|^2 \leq a'b'$ . The last condition ensures positivity of  $\rho_X$ . Taking the partial transpose with respect to subsystem  $B$ , the anti-diagonal coherence  $|00\rangle\langle 11|$  is mapped to  $|01\rangle\langle 10|$ , giving

$$\rho_X^{T_B} = \begin{pmatrix} a' & 0 & 0 & 0 \\ 0 & 0 & c' & 0 \\ 0 & c'^* & 0 & 0 \\ 0 & 0 & 0 & b' \end{pmatrix}. \quad (27)$$

This matrix decomposes into two one-dimensional blocks with eigenvalues  $a'$  and  $b'$ , and one  $2 \times 2$  block with eigenvalues  $\pm|c'|$ . Therefore,

$$\text{spec}(\rho_X^{T_B}) = \{a', b', |c'|, -|c'|\}. \quad (28)$$

**Proposition 2** (Negativity of the restricted  $X$ -state). *For any restricted  $X$ -state of the form in Eq. (26), the entanglement negativity is*

$$\mathcal{N}(\rho_X) = |c'|. \quad (29)$$

*Proof.* The only negative eigenvalue of  $\rho_X^{T_B}$  is  $-|c'|$ . Hence, using  $\mathcal{N}(\rho_X) = \sum_{\lambda_i < 0} |\lambda_i|$ , we obtain  $\mathcal{N}(\rho_X) = |c'|$ .  $\square$

This result will be used directly for the phase-damping channel, since phase damping preserves the restricted form of Eq. (26). For the global depolarizing channel, the state remains an  $X$ -state but acquires nonzero  $|01\rangle$  and  $|10\rangle$  populations. Its negativity therefore requires a separate partial-transpose calculation, carried out in Section VII.

## VI. PHASE-DAMPING CHANNEL

We first consider independent phase damping acting on both qubits after the CNOT operation. Under the

single-qubit phase-damping channel defined in Eq. (19), each single-qubit off-diagonal element is suppressed by  $\sqrt{1-p}$ , while populations remain unchanged. Therefore, the two-qubit coherence  $|00\rangle\langle 11|$ , which differs in both qubit indices, is suppressed by the product factor  $\sqrt{1-p}\sqrt{1-p} = 1-p$ .

### A. Evolved State

Starting from the CNOT output state in Eq. (12), the phase-damped state is

$$\rho_{\text{phase}} = \mathcal{E}_{\text{phase}}^{(2)}(\rho). \quad (30)$$

Since phase damping preserves populations, the diagonal elements remain  $\cos^2\theta$  and  $\sin^2\theta$ . The only nonzero off-diagonal element is transformed as follows:

$$c \mapsto c_{\text{phase}} = (1-p)c = \frac{1}{2}(1-p)e^{-i\phi} \sin(2\theta). \quad (31)$$

Thus, the evolved density matrix is

$$\rho_{\text{phase}} = \begin{pmatrix} \cos^2\theta & 0 & 0 & \frac{1}{2}(1-p)e^{-i\phi} \sin(2\theta) \\ 0 & 0 & 0 & 0 \\ 0 & 0 & 0 & 0 \\ \frac{1}{2}(1-p)e^{i\phi} \sin(2\theta) & 0 & 0 & \sin^2\theta \end{pmatrix}. \quad (32)$$

the state; therefore, it retains the restricted  $X$ -state form of Eq. (26).

### B. Negativity under Phase Damping

Because  $\rho_{\text{phase}}$  has the restricted  $X$ -state structure, Proposition 2 applies directly. The negativity is given by the magnitude of the anti-diagonal element:

$$\mathcal{N}_{\text{phase}}(\theta, p) = |c_{\text{phase}}|. \quad (33)$$

Substituting Eq. (31), we obtain the exact expression

$$\boxed{\mathcal{N}_{\text{phase}}(\theta, p) = \frac{1}{2}(1-p) \sin(2\theta)}. \quad (34)$$

This result holds for  $p \in [0, 1]$  and  $\theta \in [0, \pi/2]$ . It reduces to the ideal value  $\mathcal{N}_0(\theta) = \frac{1}{2} \sin(2\theta)$  at  $p = 0$ , and vanishes only for complete phase damping,  $p = 1$ , or for incoherent input states with  $\theta = 0$  or  $\theta = \pi/2$ .

### C. Consequences

Equation (34) shows that phase damping acts as a purely multiplicative suppression of the ideal output negativity:

$$\mathcal{N}_{\text{phase}}(\theta, p) = (1-p)\mathcal{N}_0(\theta). \quad (35)$$

Accordingly, the conversion efficiency relative to the noiseless protocol is

$$\eta_{\text{phase}}(p) = \frac{\mathcal{N}_{\text{phase}}(\theta, p)}{\mathcal{N}_0(\theta)} = 1 - p, \quad \theta \in (0, \pi/2). \quad (36)$$

The efficiency is independent of the initial coherence angle  $\theta$ . Thus, within the present parametrization, phase damping reduces the absolute amount of entanglement generated, but it does not favor one nonzero input coherence strength over another in terms of relative conversion efficiency.

A further consequence is the absence of finite- $p$  entanglement sudden death. For every  $\theta \in (0, \pi/2)$ , the negativity remains strictly positive for all  $p < 1$ . Hence, independent phase damping produces a smooth linear decay of entanglement rather than an abrupt transition to a separable state.

## VII. GLOBAL DEPOLARIZING CHANNEL

We now consider the global two-qubit depolarizing channel defined in Eq. (23). Unlike phase damping, which only suppresses off-diagonal coherences, the global depolarizing channel mixes the full two-qubit state with the maximally mixed state. This produces both a multiplicative reduction of the entanglement-carrying coherence and an additive shift of all diagonal populations toward  $1/4$ .

### A. Evolved State

Applying the global depolarizing channel to the CNOT output state  $\rho$  gives

$$\begin{aligned} \rho_{\text{dep}} = \mathcal{E}_{\text{dep}}(\rho) &= (1-p)\rho + \frac{p}{4}\mathbb{I}_4 \\ &= \begin{pmatrix} (1-p)\cos^2\theta + \frac{p}{4} & 0 & 0 & \frac{1}{2}(1-p)e^{-i\phi}\sin(2\theta) \\ 0 & \frac{p}{4} & 0 & 0 \\ 0 & 0 & \frac{p}{4} & 0 \\ \frac{1}{2}(1-p)e^{i\phi}\sin(2\theta) & 0 & 0 & (1-p)\sin^2\theta + \frac{p}{4} \end{pmatrix}. \end{aligned} \quad (37)$$

Equivalently, using  $a = \cos^2\theta$ ,  $b = \sin^2\theta$ , and  $c = \frac{1}{2}e^{-i\phi}\sin(2\theta)$ , this state has diagonal elements  $(1-p)a + p/4$ ,  $p/4$ ,  $p/4$ , and  $(1-p)b + p/4$ , while the anti-diagonal coherence becomes

$$c_{\text{dep}} = (1-p)c = \frac{1}{2}(1-p)e^{-i\phi}\sin(2\theta). \quad (38)$$

Thus, the depolarizing channel preserves the  $X$ -state structure but not the restricted form used in Proposition 2, because the  $|01\rangle$  and  $|10\rangle$  populations are now nonzero.

### B. Partial Transpose Spectrum

Taking the partial transpose with respect to subsystem  $B$ , the anti-diagonal entries  $|00\rangle\langle 11|$  and  $|11\rangle\langle 00|$  are moved to the  $|01\rangle\langle 10|$  and  $|10\rangle\langle 01|$  positions. Hence,

$$\rho_{\text{dep}}^{T_B} = \begin{pmatrix} (1-p)a + \frac{p}{4} & 0 & 0 & 0 \\ 0 & \frac{p}{4} & (1-p)c & 0 \\ 0 & (1-p)c^* & \frac{p}{4} & 0 \\ 0 & 0 & 0 & (1-p)b + \frac{p}{4} \end{pmatrix}. \quad (39)$$

This matrix is block diagonal. Two eigenvalues are read off directly:

$$\lambda_1 = (1-p)a + \frac{p}{4}, \quad \lambda_2 = (1-p)b + \frac{p}{4}. \quad (40)$$

The remaining two eigenvalues come from the central  $2 \times 2$  block,

$$\begin{pmatrix} \frac{p}{4} & (1-p)c \\ (1-p)c^* & \frac{p}{4} \end{pmatrix}, \quad (41)$$

which has eigenvalues

$$\lambda_{\pm} = \frac{p}{4} \pm (1-p)|c|. \quad (42)$$

Using  $|c| = \frac{1}{2}\sin(2\theta)$ , these become

$$\lambda_{\pm} = \frac{p}{4} \pm \frac{1}{2}(1-p)\sin(2\theta). \quad (43)$$

The eigenvalues  $\lambda_1$ ,  $\lambda_2$ , and  $\lambda_+$  are non-negative for all  $p \in [0, 1]$ . The only eigenvalue that can become negative is

$$\lambda_- = \frac{p}{4} - \frac{1}{2}(1-p)\sin(2\theta). \quad (44)$$

### C. Negativity under Global Depolarizing Noise

The negativity is the absolute value of the negative part of the partial-transpose spectrum. Since only  $\lambda_-$  can be negative, we obtain

$$\mathcal{N}_{\text{dep}}(\theta, p) = \max(0, -\lambda_-). \quad (45)$$

Substituting Eq. (44) gives the exact expression

$$\mathcal{N}_{\text{dep}}(\theta, p) = \max\left[0, \frac{1}{2}(1-p)\sin(2\theta) - \frac{p}{4}\right]. \quad (46)$$

At  $p = 0$ , this reduces to the ideal negativity  $\mathcal{N}_0(\theta) = \frac{1}{2}\sin(2\theta)$ . As  $p$  increases, the first term decreases because the entanglement-carrying coherence is suppressed by  $(1-p)$ , while the second term arises from the isotropic mixing with  $\mathbb{I}_4/4$ . When these two contributions become equal, the negative eigenvalue of the partial transpose reaches zero and the state becomes separable. This mechanism gives rise to entanglement sudden death, analyzed in the next section.

## VIII. ENTANGLEMENT SUDDEN DEATH UNDER GLOBAL DEPOLARIZING NOISE

The expression in Eq. (46) shows that global depolarizing noise can completely suppress the entanglement generated by the CNOT gate at a finite noise strength. This finite-noise disappearance of entanglement is the entanglement sudden-death effect. In the present protocol, it occurs when the only potentially negative eigenvalue of  $\rho_{\text{dep}}^{T_B}$  reaches zero.

### A. Critical Depolarizing Strength

The sudden-death threshold  $p_c$  is obtained by setting  $\lambda_- = 0$  in Eq. (44). Thus,

$$\frac{p_c}{4} = \frac{1}{2}(1 - p_c) \sin(2\theta). \quad (47)$$

Solving for  $p_c$  gives

$$p_c(\theta) = \frac{2 \sin(2\theta)}{2 \sin(2\theta) + 1}. \quad (48)$$

For  $p < p_c(\theta)$ , the partial transpose has one negative eigenvalue and the output state is entangled. For  $p \geq p_c(\theta)$ , all eigenvalues of the partial transpose are non-negative, and the two-qubit state is separable.

For the maximally coherent input,  $\theta = \pi/4$ , one has  $\sin(2\theta) = 1$ , and therefore

$$p_c\left(\frac{\pi}{4}\right) = \frac{2}{3}. \quad (49)$$

In this case, the CNOT output before noise is a Bell state, and the depolarized state reduces to the standard depolarized Bell-state mixture. The threshold  $p_c = 2/3$  is therefore consistent with the known separability boundary for this class of two-qubit states.

**Theorem 3** (Entanglement sudden death). *Under the global two-qubit depolarizing channel  $\mathcal{E}_{\text{dep}}(\rho) = (1-p)\rho + p\mathbb{1}_4/4$ , any input with nonzero coherence,  $\theta \in (0, \pi/2)$ , has a finite critical noise strength  $p_c(\theta) \in (0, 1)$  such that  $\mathcal{N}_{\text{dep}}(\theta, p) > 0$  for  $p < p_c(\theta)$  and  $\mathcal{N}_{\text{dep}}(\theta, p) = 0$  for  $p \geq p_c(\theta)$ .*

*Proof.* For  $\theta \in (0, \pi/2)$ , we have  $\sin(2\theta) > 0$ . Hence Eq. (48) implies

$$0 < p_c(\theta) = \frac{2 \sin(2\theta)}{2 \sin(2\theta) + 1} < 1.$$

From Eq. (46), the negativity is positive exactly when  $\frac{1}{2}(1-p) \sin(2\theta) - \frac{p}{4} > 0$ , which is equivalent to  $p < p_c(\theta)$ . For  $p \geq p_c(\theta)$ , the negative eigenvalue of the partial transpose is lifted to zero or positive values, and the negativity vanishes.  $\square$

**Corollary 4** (Dependence on input coherence). *The critical noise strength  $p_c(\theta)$  is a monotonically increasing function of  $\sin(2\theta)$ . It reaches its maximum value  $2/3$  at  $\theta = \pi/4$  and approaches zero as  $\theta \rightarrow 0$  or  $\theta \rightarrow \pi/2$ .*

*Proof.* Let  $x = \sin(2\theta)$ , with  $x \in [0, 1]$ . Then

$$p_c(x) = \frac{2x}{2x + 1}.$$

Differentiating gives

$$\frac{dp_c}{dx} = \frac{2}{(2x + 1)^2} > 0.$$

Thus,  $p_c$  increases monotonically with  $x = \sin(2\theta)$ . Since  $\sin(2\theta)$  is maximal at  $\theta = \pi/4$ , the largest threshold is  $p_c = 2/3$ . As  $\theta \rightarrow 0$  or  $\theta \rightarrow \pi/2$ ,  $x \rightarrow 0$ , and hence  $p_c \rightarrow 0$ .  $\square$

This result shows that larger input coherence produces entanglement that is more robust against global depolarizing noise. In contrast, weakly coherent inputs generate weak entanglement that is destroyed by arbitrarily small amounts of depolarizing noise in the limit  $\theta \rightarrow 0$  or  $\theta \rightarrow \pi/2$ .

### B. Comparison with Phase Damping

The sudden-death behavior is specific to the global depolarizing channel. For independent phase damping, the negativity is  $\mathcal{N}_{\text{phase}}(\theta, p) = \frac{1}{2}(1-p) \sin(2\theta)$ . Therefore, for every  $\theta \in (0, \pi/2)$ , one has  $\mathcal{N}_{\text{phase}}(\theta, p) > 0$  for all  $p < 1$ . Entanglement vanishes only at complete phase damping,  $p = 1$ , rather than at a finite threshold.

The qualitative difference arises from the structure of the noise. Phase damping only suppresses the off-diagonal element carrying the entanglement, so the negative eigenvalue of the partial transpose approaches zero smoothly. Global depolarization, however, both suppresses this coherence and adds an isotropic identity component. The identity component shifts the partial-transpose spectrum upward by  $p/4$ , allowing the negative eigenvalue to cross zero at the finite threshold  $p_c(\theta)$ .

## IX. CONVERSION EFFICIENCY

We now quantify the fraction of ideal CNOT-generated entanglement that survives after the noise channel. Since the ideal output negativity is  $\mathcal{N}_0(\theta) = \frac{1}{2} \sin(2\theta)$ , we define the coherence-to-entanglement conversion efficiency as

$$\eta(\theta, p) = \frac{\mathcal{N}(\theta, p)}{\mathcal{N}_0(\theta)} = \frac{\mathcal{N}(\theta, p)}{\frac{1}{2} \sin(2\theta)}. \quad (50)$$

This quantity is defined for  $\theta \in (0, \pi/2)$ , where the input has nonzero  $l_1$ -norm coherence and  $\mathcal{N}_0(\theta) > 0$ . The efficiency is normalized so that  $\eta = 1$  in the noiseless case

and  $\eta = 0$  when the output state is separable. Since the normalization uses negativity, the numerical value of  $\eta$  should be understood relative to negativity as the chosen entanglement measure.

### A. Phase-Damping Efficiency

For independent phase damping, the negativity is  $\mathcal{N}_{\text{phase}}(\theta, p) = (1 - p)\mathcal{N}_0(\theta)$ . Substituting into Eq. (50) gives

$$\boxed{\eta_{\text{phase}}(p) = 1 - p}. \quad (51)$$

Thus, within the phase-damping parametrization used in this work, the conversion efficiency is independent of the initial coherence strength. Changing  $\theta$  changes the absolute amount of entanglement generated, through  $\mathcal{N}_0(\theta)$ , but it does not change the fraction that survives phase damping. This reflects the purely multiplicative action of phase damping on the entanglement-carrying coherence  $|00\rangle\langle 11|$ .

### B. Global Depolarizing Efficiency

For the global two-qubit depolarizing channel, substituting Eq. (46) into Eq. (50) yields

$$\boxed{\eta_{\text{dep}}(\theta, p) = \max\left[0, (1 - p) - \frac{p}{2 \sin(2\theta)}\right]}. \quad (52)$$

Unlike the phase-damping case, the depolarizing efficiency depends explicitly on the input coherence through  $\sin(2\theta)$ . For fixed noise strength  $p$ , inputs with larger coherence retain a larger fraction of their ideal output negativity. Conversely, weakly coherent inputs have small ideal negativity and are more easily driven to zero entanglement by the isotropic mixing term.

The efficiency vanishes when

$$(1 - p) - \frac{p}{2 \sin(2\theta)} = 0, \quad (53)$$

which gives the same sudden-death threshold derived in Eq. (48),

$$p_c(\theta) = \frac{2 \sin(2\theta)}{2 \sin(2\theta) + 1}. \quad (54)$$

Therefore, the efficiency picture is consistent with the partial-transpose analysis: global depolarizing noise not only reduces the output entanglement but also imposes a coherence-dependent finite threshold beyond which the conversion efficiency is exactly zero.

### C. Comparison of the Two Channels

The two efficiencies summarize the different degradation mechanisms:

$$\eta_{\text{phase}}(p) = 1 - p, \quad (55)$$

$$\eta_{\text{dep}}(\theta, p) = \max\left[0, (1 - p) - \frac{p}{2 \sin(2\theta)}\right]. \quad (56)$$

Phase damping produces a universal linear reduction of the conversion efficiency, independent of the initial coherence angle. Global depolarization produces a coherence-dependent efficiency and a finite sudden-death threshold. Hence, maximizing the initial coherence  $\sin(2\theta)$  not only maximizes the ideal output negativity, but also maximizes the robustness of the conversion against global depolarizing noise.

## X. SUMMARY OF EXACT ANALYTIC RESULTS

We summarize the closed-form results obtained above. For the ideal CNOT conversion protocol, the output negativity is

$$\mathcal{N}_0(\theta) = \frac{1}{2} \sin(2\theta) = \frac{1}{2} C_{l_1}(|\psi_A\rangle). \quad (57)$$

Thus, in the absence of noise, the CNOT gate converts the input  $l_1$ -norm coherence into bipartite entanglement with a proportionality factor  $1/2$  when entanglement is quantified by negativity.

For independent phase damping on both qubits, with the parametrization of Eq. (19), the negativity is

$$\mathcal{N}_{\text{phase}}(\theta, p) = \frac{1}{2} (1 - p) \sin(2\theta), \quad (58)$$

and the corresponding conversion efficiency is

$$\eta_{\text{phase}}(p) = 1 - p. \quad (59)$$

The efficiency is independent of the initial coherence angle  $\theta$ .

For the global two-qubit depolarizing channel, the negativity is

$$\mathcal{N}_{\text{dep}}(\theta, p) = \max\left[0, \frac{1}{2} (1 - p) \sin(2\theta) - \frac{p}{4}\right], \quad (60)$$

with conversion efficiency

$$\eta_{\text{dep}}(\theta, p) = \max\left[0, (1 - p) - \frac{p}{2 \sin(2\theta)}\right], \quad \theta \in (0, \pi/2). \quad (61)$$

The associated entanglement sudden-death threshold is

$$p_c(\theta) = \frac{2 \sin(2\theta)}{2 \sin(2\theta) + 1}. \quad (62)$$

For the maximally coherent input,  $\theta = \pi/4$ , this gives  $p_c = 2/3$ .

Equations (57)–(62) provide a compact description of the two degradation regimes considered in this work: phase damping produces universal multiplicative suppression, whereas global depolarization produces coherence-dependent decay with finite-threshold entanglement sudden death.

## XI. NUMERICAL VALIDATION

We verify the analytic expressions by direct density-matrix simulation of the full two-qubit protocol. Although the preceding derivations are exact, the numerical calculation provides an independent consistency check of the channel implementations and the partial-transpose spectra.

### A. Simulation Method

The simulated protocol is

$$\rho_{\text{out}} = \mathcal{E}_{\text{noise}} \left( U_{\text{CNOT}} \rho_0 U_{\text{CNOT}}^\dagger \right), \quad (63)$$

where  $\rho_0 = \rho_A \otimes |0\rangle\langle 0|$ , and  $\mathcal{E}_{\text{noise}}$  is either independent phase damping on both qubits or the global two-qubit depolarizing channel.

For phase damping, the channel is implemented using the two-qubit Kraus operators  $K_{ij} = K_i \otimes K_j$ , with  $K_i$  defined in Eq. (19). The output state is computed as

$$\rho_{\text{phase}} = \sum_{i,j=0}^1 K_{ij} \rho K_{ij}^\dagger. \quad (64)$$

For the global depolarizing channel, the output state is computed directly from

$$\rho_{\text{dep}} = (1-p)\rho + \frac{p}{4}\mathbb{I}_4. \quad (65)$$

At each parameter point  $(\theta, p)$ , the partial transpose with respect to subsystem  $B$  is formed explicitly, and its eigenvalues are computed using a Hermitian eigensolver. The numerical negativity is then obtained from

$$\mathcal{N}_{\text{num}} = \sum_{\lambda_i < 0} |\lambda_i|, \quad (66)$$

where  $\{\lambda_i\}$  are the eigenvalues of  $\rho_{\text{out}}^{T_B}$ .

### B. Parameter Grid and Error Measure

The numerical calculations are performed on a uniform grid over  $\theta \in [0.01, \pi/2]$  and  $p \in [0, 1]$ . The lower endpoint  $\theta = 0.01$  is used instead of  $\theta = 0$  when computing efficiencies, because the ideal negativity vanishes at

$\theta = 0$ . Additional one-dimensional checks are performed at fixed  $\theta = \pi/4$ , corresponding to a maximally coherent input.

The numerical results are compared with the analytic expressions  $\mathcal{N}_{\text{phase}}(\theta, p)$  and  $\mathcal{N}_{\text{dep}}(\theta, p)$  derived in Eqs. (34) and (46). The maximum absolute deviation is quantified as

$$\Delta_{\text{max}} = \max_{\theta, p} |\mathcal{N}_{\text{num}}(\theta, p) - \mathcal{N}_{\text{analytic}}(\theta, p)|. \quad (67)$$

Across the full parameter grid, we find

$$\Delta_{\text{max}} < 10^{-12}, \quad (68)$$

with residuals consistent with double-precision floating-point roundoff. This agreement confirms both the analytic expressions and the numerical implementation of the noise channels.

### C. Numerical Results

Figure 1 shows the output negativity as a function of the noise strength  $p$  for the maximally coherent input  $\theta = \pi/4$ . The phase-damping curve decreases linearly and vanishes only at  $p = 1$ , whereas the global depolarizing curve reaches zero at the sudden-death threshold  $p_c = 2/3$ . The numerical data agree with the analytic expressions within the numerical precision reported above.

Figure 2 shows the negativity as a function of the input coherence angle  $\theta$  for representative noise strengths. The curves follow the expected  $\sin(2\theta)$  dependence in the ideal and phase-damped cases, while the depolarizing channel exhibits a thresholded response due to the  $\max(0, \cdot)$  structure of Eq. (46).

Figure 3 compares the conversion efficiencies  $\eta_{\text{phase}}$  and  $\eta_{\text{dep}}$  at  $\theta = \pi/4$ . The phase-damping efficiency follows the universal linear law  $1 - p$ , while the depolarizing efficiency vanishes at the finite threshold  $p_c = 2/3$ .

Figure 4 presents the two-dimensional negativity landscape over the  $(\theta, p)$  parameter space for both noise channels. For phase damping, the negativity decreases smoothly with  $p$  and remains positive for all  $p < 1$  whenever  $\theta \in (0, \pi/2)$ . For global depolarizing noise, the analytic sudden-death boundary  $p_c(\theta)$  separates the entangled and separable regions.

Figure 5 shows the depolarizing sudden-death threshold extracted from the numerical simulations and compares it with the analytic expression in Eq. (48). The threshold is maximal for the maximally coherent input and approaches zero as the input coherence vanishes.

Finally, Fig. 6 illustrates the ideal coherence–entanglement relation. The input  $l_1$ -norm coherence is  $C_{l_1} = \sin(2\theta)$ , while the noiseless output negativity is  $\mathcal{N}_0 = \frac{1}{2} \sin(2\theta)$ . The numerical calculation therefore confirms the proportionality  $\mathcal{N}_0 = \frac{1}{2} C_{l_1}$ .

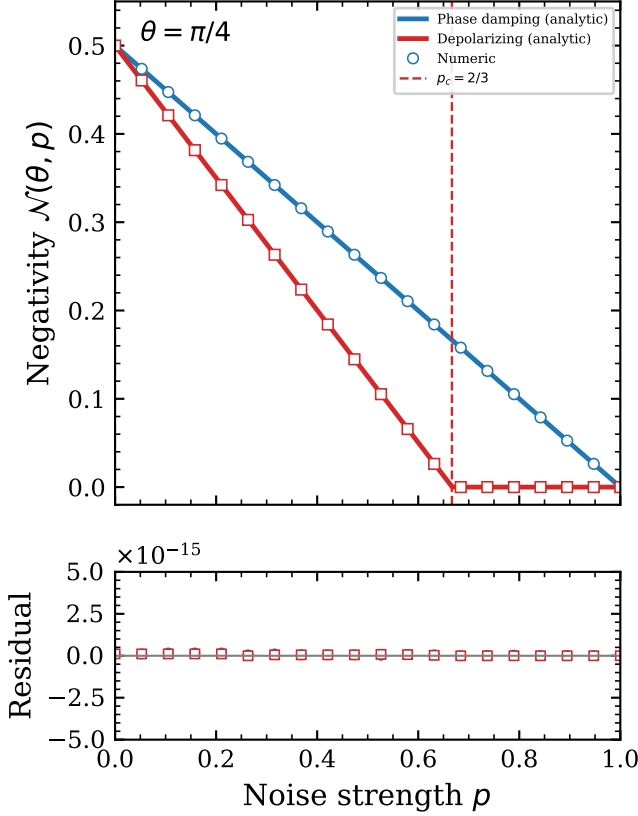


FIG. 1. Entanglement negativity  $\mathcal{N}(\theta, \rho)$  as a function of noise strength  $\rho$  for the maximally coherent input  $\theta = \pi/4$ . Solid curves denote the analytic expressions in Eqs. (34) and (46), while symbols denote direct numerical simulation. The vertical dashed line marks the depolarizing sudden-death threshold  $\rho_c = 2/3$ .

## XII. DISCUSSION

The results above provide a simple analytic picture of how local coherence is converted into bipartite entanglement by a CNOT gate and how this conversion is affected by different noise mechanisms. In the noiseless protocol, the input  $l_1$ -norm coherence  $C_{l_1}(|\psi_A\rangle) = \sin(2\theta)$  is mapped into output negativity according to  $\mathcal{N}_0 = \frac{1}{2}C_{l_1}$ . This relation gives a direct quantitative link between the local resource initially present in qubit  $A$  and the non-local resource generated between qubits  $A$  and  $B$ , with the factor  $1/2$  arising from the use of negativity as the entanglement measure.

The two noise channels considered here modify this conversion in qualitatively different ways. Independent phase damping suppresses the off-diagonal element  $|00\rangle\langle 11|$ , which is the only coherence responsible for entanglement in the CNOT-generated state. Since the populations are unchanged, the partial-transpose spectrum retains the same structure as in the noiseless case, with the negative eigenvalue scaled smoothly by the factor  $1 - p$ . As a result, the negativity becomes  $\mathcal{N}_{\text{phase}} =$

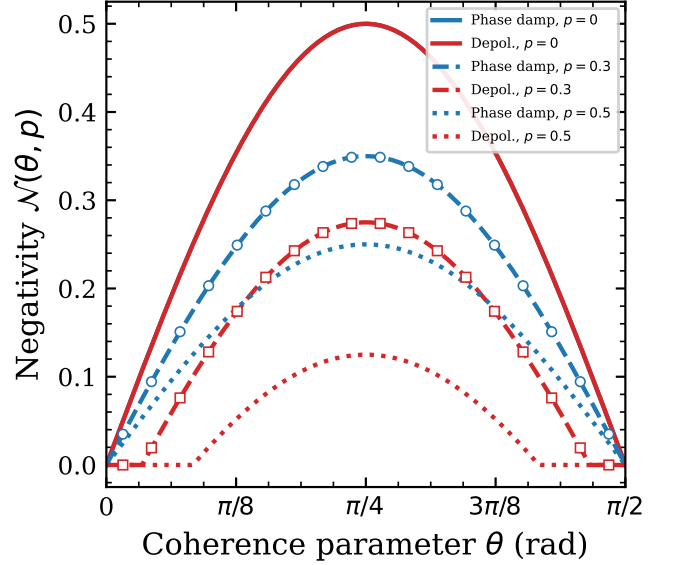


FIG. 2. Entanglement negativity  $\mathcal{N}(\theta, \rho)$  as a function of the input coherence angle  $\theta$  for representative noise strengths. Phase damping preserves the  $\sin(2\theta)$  profile up to a multiplicative factor, whereas global depolarizing noise introduces a threshold through the term  $-p/4$  in Eq. (46). Symbols denote numerical simulations.

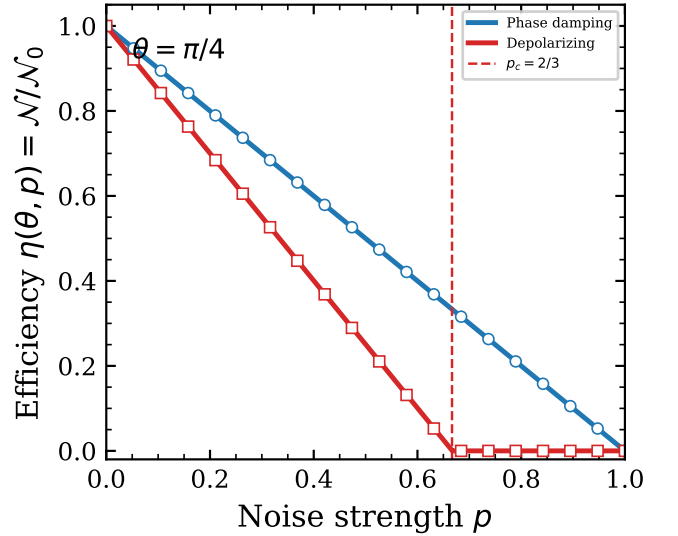


FIG. 3. Coherence-to-entanglement conversion efficiency  $\eta(\theta, \rho) = \mathcal{N}(\theta, \rho)/\mathcal{N}_0(\theta)$  for  $\theta = \pi/4$ . The phase-damping efficiency is  $\eta_{\text{phase}} = 1 - p$ , while the global depolarizing efficiency decreases to zero at  $\rho_c = 2/3$ . Symbols denote numerical simulations.

$(1 - p)\mathcal{N}_0$ , and entanglement vanishes only at complete phase damping,  $p = 1$ , for any nonzero input coherence.

Global depolarizing noise acts differently. It also suppresses the entanglement-carrying coherence by the factor  $1 - p$ , but in addition it mixes the state with  $\mathbb{I}_4/4$ . This isotropic mixing shifts the partial-transpose eigen-

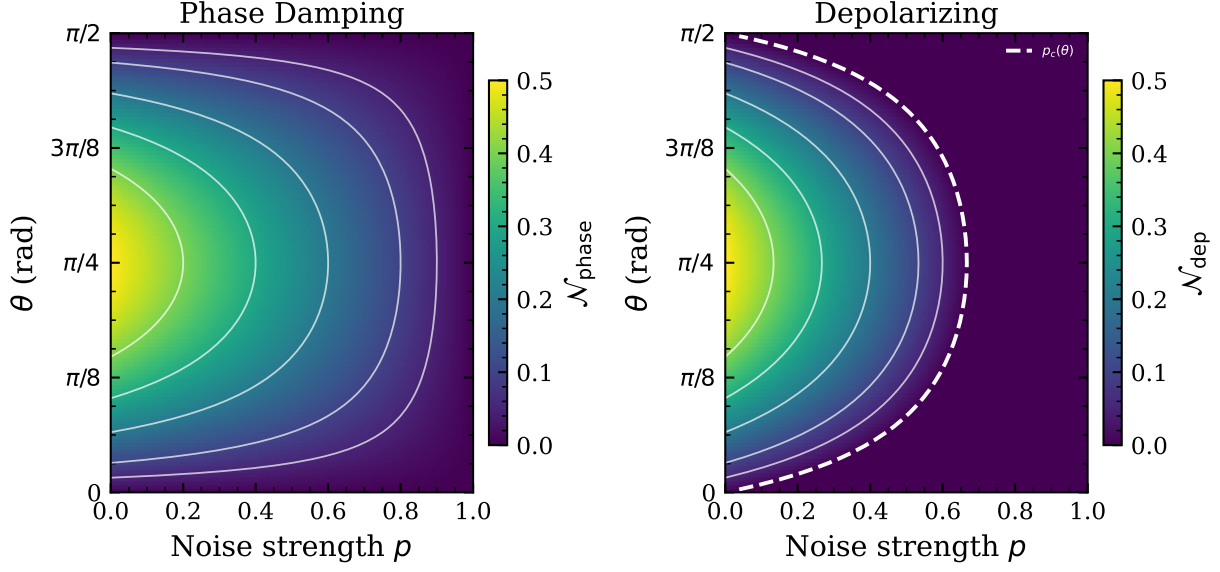


FIG. 4. Two-dimensional negativity landscape  $\mathcal{N}(\theta, p)$  over the full  $(\theta, p)$  parameter space for independent phase damping and global depolarizing noise. Contours show analytic negativity levels. In the depolarizing case, the dashed curve marks the analytic sudden-death boundary  $p_c(\theta) = 2 \sin(2\theta) / [2 \sin(2\theta) + 1]$ .

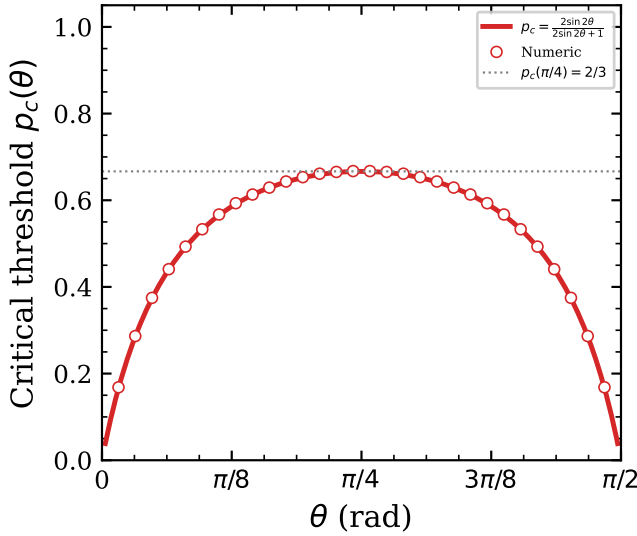


FIG. 5. Entanglement sudden-death threshold  $p_c(\theta)$  for the global two-qubit depolarizing channel. The solid curve is the analytic result in Eq. (48), while symbols denote thresholds extracted numerically from the first zero of  $\mathcal{N}_{\text{dep}}(\theta, p)$ . The maximum value  $p_c = 2/3$  occurs at  $\theta = \pi/4$ .

values upward by  $p/4$ . The negative eigenvalue therefore reaches zero at a finite noise strength, producing entanglement sudden death. The resulting threshold  $p_c(\theta) = 2 \sin(2\theta) / [2 \sin(2\theta) + 1]$  depends on the initial coherence: larger input coherence generates stronger entanglement and hence survives to larger depolarizing strengths. For the maximally coherent input, the threshold becomes  $p_c = 2/3$ , in agreement with the known sep-

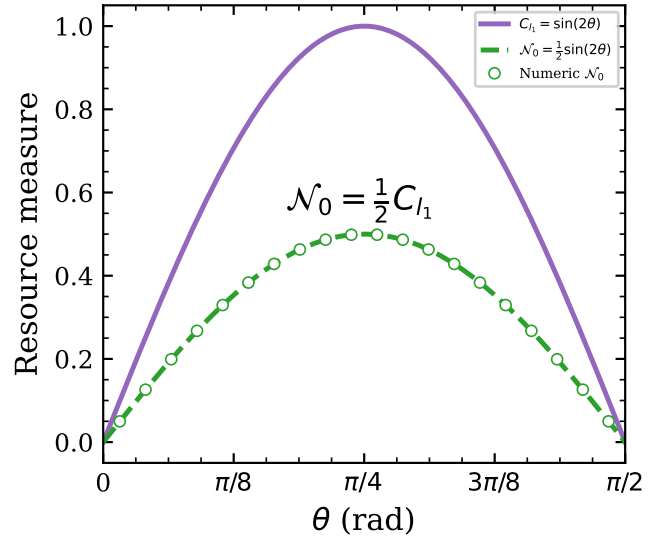


FIG. 6. Ideal coherence–entanglement relation in the noiseless CNOT protocol. The  $l_1$ -norm coherence of the input is  $C_{l_1} = \sin(2\theta)$ , while the output negativity is  $\mathcal{N}_0 = \frac{1}{2} \sin(2\theta)$ . Symbols denote numerical negativity values, confirming  $\mathcal{N}_0 = \frac{1}{2} C_{l_1}$ .

arability boundary of the depolarized Bell-state mixture.

This contrast can be summarized in terms of conversion efficiency. For phase damping,  $\eta_{\text{phase}} = 1 - p$ , independent of  $\theta$ . Thus, changing the input coherence changes the absolute amount of generated entanglement but not the fraction that survives dephasing. For global depolarization, however,  $\eta_{\text{dep}} = \max[0, (1 - p) - p / (2 \sin(2\theta))]$ , which explicitly depends on the input co-

herence. In this case, choosing the maximally coherent input  $\theta = \pi/4$  is optimal in two senses: it maximizes the ideal output negativity and also maximizes the sudden-death threshold.

The distinction between the two channels reflects the different ways in which they alter the partial-transpose spectrum. Phase damping only reduces the magnitude of the off-diagonal coherence and therefore drives the negative eigenvalue continuously toward zero. Global depolarization, by contrast, combines coherence suppression with an additive identity component, which can eliminate the negative eigenvalue at a finite value of  $p$ . Thus, even though both channels reduce the same anti-diagonal coherence, their effects on entanglement are not equivalent.

These results also provide a useful benchmark for near-term quantum devices. Entanglement generation by CNOT-type gates is a basic component of many quantum circuits, and the ability to distinguish smooth dephasing-like decay from depolarizing-induced sudden death can help interpret effective noise models at the circuit level. The present analysis is deliberately idealized: the CNOT operation itself is assumed perfect, the noise is applied after the gate, and only two Markovian one-parameter channels are considered. Real devices may involve local depolarization, amplitude damping, coherent control errors, leakage, crosstalk, non-Markovian effects, and measurement imperfections. Nevertheless, the closed-form expressions derived here offer a transparent reference point against which more detailed hardware-specific models can be compared.

The analysis further illustrates the usefulness of restricted  $X$ -state structure in obtaining analytic results. Because the CNOT-generated state has support only in the  $\{|00\rangle, |11\rangle\}$  subspace, both the phase-damping and global depolarizing channels preserve an  $X$ -state form. This makes the partial-transpose spectrum tractable and allows the entanglement behavior to be traced directly to a single potentially negative eigenvalue. Extensions to more general input states, additional noise channels, or multi-qubit CNOT networks may not retain this simple structure, but the present two-qubit protocol provides a useful baseline for such generalizations.

### XIII. CONCLUSION

We have analysed coherence-to-entanglement conversion in a minimal two-qubit CNOT protocol under two canonical noise models: independent phase damping on both qubits and a global two-qubit depolarizing channel. Starting from a coherent single-qubit input  $|\psi_A\rangle = \cos\theta|0\rangle + e^{i\phi}\sin\theta|1\rangle$  and an incoherent ancilla  $|0\rangle$ , the CNOT gate generates the two-qubit state  $\cos\theta|00\rangle + e^{i\phi}\sin\theta|11\rangle$ . For the noiseless protocol, the output negativity satisfies  $\mathcal{N}_0 = \frac{1}{2}C_{l_1}$ , establishing a direct relation between the input  $l_1$ -norm coherence and the generated bipartite entanglement, with the factor  $1/2$  determined by the use of negativity as the entanglement measure.

For independent phase damping, we derived the exact negativity  $\mathcal{N}_{\text{phase}}(\theta, p) = \frac{1}{2}(1-p)\sin(2\theta)$ . This channel produces a universal multiplicative suppression of the ideal output negativity, giving the conversion efficiency  $\eta_{\text{phase}} = 1-p$ , independent of the initial coherence angle  $\theta$ . Consequently, for every nonzero input coherence, entanglement persists for all  $p < 1$  and vanishes only at complete phase damping.

For the global two-qubit depolarizing channel, we obtained  $\mathcal{N}_{\text{dep}}(\theta, p) = \max[0, \frac{1}{2}(1-p)\sin(2\theta) - p/4]$ . In contrast to phase damping, global depolarization introduces an additive identity component that shifts the partial-transpose spectrum and leads to entanglement sudden death at the finite threshold  $p_c(\theta) = 2\sin(2\theta)/[2\sin(2\theta) + 1]$ . For a maximally coherent input,  $\theta = \pi/4$ , this gives  $p_c = 2/3$ , consistent with the known separability boundary of the depolarized Bell-state mixture.

The comparison between the two channels reveals two distinct degradation mechanisms. Phase damping reduces the entanglement-carrying coherence smoothly and multiplicatively, whereas global depolarization both suppresses this coherence and shifts the partial-transpose eigenvalues through isotropic mixing. These different spectral effects lead respectively to smooth decay without finite-threshold sudden death and to coherence-dependent sudden death.

Direct density-matrix simulations confirm the closed-form expressions to double-precision accuracy. The results therefore provide a compact analytic benchmark for noise-limited coherence-to-entanglement conversion in an elementary CNOT-based protocol. Future extensions could analyze other noise models, including local depolarizing noise, amplitude damping, noisy CNOT gates, non-Markovian dynamics, multi-qubit CNOT networks, and hardware-specific noise models.

- 
- [1] M. A. Nielsen and I. L. Chuang, *Quantum Computation and Quantum Information* (Cambridge University Press, Cambridge, 2010).
- [2] R. Horodecki, P. Horodecki, M. Horodecki, and K. Horodecki, Quantum entanglement, *Reviews of Modern Physics* **81**, 865 (2009).

- [3] T. Baumgratz, M. Cramer, and M. B. Plenio, Quantifying coherence, *Physical Review Letters* **113**, 140401 (2014), arXiv:1311.0275 [quant-ph].
- [4] A. Streltsov, G. Adesso, and M. B. Plenio, Colloquium: Quantum coherence as a resource, *Reviews of Modern Physics* **89**, 041003 (2017).

- [5] M. Naseri, T. V. Kondra, S. Goswami, M. Fellous-Asiani, and A. Streltsov, Entanglement and coherence in the bernstein–vazirani algorithm, *Physical Review A* **106**, 062429 (2022).
- [6] H.-L. Shi, S.-Y. Liu, X.-H. Wang, W.-L. Yang, Z.-Y. Yang, and H. Fan, Coherence depletion in the grover quantum search algorithm, *Physical Review A* **95**, 032307 (2017).
- [7] C. Feng, L. Chen, and L.-J. Zhao, Coherence and entanglement in grover and harrow–hassidim–lloyd algorithm, *Physica A: Statistical Mechanics and its Applications* **626**, 129048 (2023).
- [8] Y.-C. Liu, J. Shang, and X. Zhang, Coherence depletion in quantum algorithms, *Entropy* **21**, 260 (2019).
- [9] F. Ahnefeld, T. Theurer, D. Egloff, J. M. Matera, and M. B. Plenio, Coherence as a resource for shor’s algorithm, *Physical Review Letters* **129**, 120501 (2022).
- [10] L. Ye, Z. Wu, and S.-M. Fei, Coherence and entanglement dynamics in shor’s algorithm, *Communications in Theoretical Physics* **78**, 015102 (2026), [arXiv:2604.06639 \[quant-ph\]](https://arxiv.org/abs/2604.06639).
- [11] A. Streltsov, U. Singh, H. S. Dhar, M. N. Bera, and G. Adesso, Measuring quantum coherence with entanglement, *Physical Review Letters* **115**, 020403 (2015).
- [12] A. A. Clerk, M. H. Devoret, S. M. Girvin, F. Marquardt, and R. J. Schoelkopf, Introduction to quantum noise, measurement, and amplification, *Reviews of Modern Physics* **82**, 1155 (2010).
- [13] D. Suter and G. A. Álvarez, Colloquium: Protecting quantum information against environmental noise, *Reviews of Modern Physics* **88**, 041001 (2016).
- [14] T. Yu and J. H. Eberly, Quantum open system theory: Bipartite aspects, *Physical Review Letters* **97**, 140403 (2006).
- [15] G. Vidal and R. F. Werner, Computable measure of entanglement, *Physical Review A* **65**, 032314 (2002), [arXiv:quant-ph/0102117](https://arxiv.org/abs/quant-ph/0102117).
- [16] M. B. Plenio and S. Virmani, An introduction to entanglement measures, *Quantum Information and Computation* **7**, 1 (2007), [arXiv:quant-ph/0504163](https://arxiv.org/abs/quant-ph/0504163).